Dimension Reduction in Pattern Forming Systems with Heterogeneous Connection Topologies

Viktor K. Jirsa*)

Center for Complex Systems & Brain Sciences, Florida Atlantic University
777 Glades Road, Boca Raton, FL 33431, USA

Spatiotemporal pattern formation in physical and chemical systems is typically based on a dynamics with a homogeneous, i.e. translationally invariant, connection topology. However, biological systems like the human cortex show homogeneous connectivity with additional strongly heterogeneous projections from one area to another. Here we use nonlinear retarded integral equations to describe the spatiotemporal dynamics of systems with heterogeneous connections. Systematic changes in the connection topology may be used as a control parameter to guide the system through a series of phase transitions. Here we show how the dynamics of the entire system may be reduced to a few degrees of freedom at these bifurcation points.

§1. Introduction

Coherent pattern formation and self-organization on macroscopic scales has been mainly the domain of partial differential equations (PDEs). External control parameters guide the system dynamics through bifurcations from one state to another. Many examples can be found in physics, e.g. hydrodynamics, laser, and chemistry, e.g. Belousov Zhabotinsky reaction (see Refs. 1), 2) for reviews). The connection topology of the underlying material substrate is exclusively homogeneous in the sense of space invariance. To the extent that inhomogeneous properties are considered, they are typically introduced as spatially varying parameters or inputs to the homogeneous system (see e.g. Ref. 3) for a recent example). On the other hand, biological systems such as the brain often have a connectivity which is spatially variant. In such cases, a description of the dynamics as a PDE results in high order differentials and a multitude of delays raising the complexity enormously. An integral description, however, allows for spatiotemporal pattern formation and provides a simpler representation and control of the inhomogeneous connection topology by its integral kernel. A first attempt of a treatment of an inhomogeneous connection topology in a dynamic system has been made by the introduction of an instantaneous long-range connection between areas in a discretely coupled chain of oscillators.[4)] Jirsa et al.[5)] report an integral formulation of a spatially continuous dynamic system with a heterogeneous connection topology and propagation delays along its connections. In §2 we briefly report a formalism[6)] which allows such a system's analytic treatment of pattern formation by means of a mode decomposition. Note that for the first time a topological control parameter has been introduced to a continuous dynamic system for the control of its macroscopic spatiotemporal dynamics.[5),6)] In §3 the paradigmatic example of a two-point connection embedded in a continu-

*) E-mail address: jirsa@walt.ccs.fau.edu

ous homogeneously connected medium illustrates the destabilization mechanism of a heterogeneous connection. The destabilization leads to a non-equilibrium phase transition of the macroscopic dynamics of the entire system, but is governed only by a few degrees of freedom. In §4 we show how its dynamics described by nonlinear retarded integral equations can be reduced to a low-dimensional description invoking Haken's enslaving principle. [1]

§2. Analytical treatment of integral equations

We define the spatiotemporal dynamics of a scalar field $\psi(x,t)$ with space $x \in \mathcal{R}^n$ and time $t \in \mathcal{R}$ as a nonlinear retarded integral equation of the form

$$\psi(x,t) = \int_A dX f(x,X) S(\psi(X,T) + I(X,T)), \tag{2·1}$$

where $f(x,X)$ describes a general connectivity function and S a nonlinear function of ψ at space-point X and a time-point $T = t - |x-X|/v$ delayed by the propagation time over the distance $|x - X|$. A denotes the surface area of the medium and v the constant signal velocity. $I(t)$ is the input to the field $\psi(x,t)$. Variations of this type of integral equation have been widely used in theoretical neuroscience [7)-11)] to describe the dynamics of neural activity. But in all these cases, as well as generally in physical systems, translational variance $f(x,X) = f(|x-X|)$ has been employed. Here we assume $f(x,X)$ to be a general function of x and X. We decompose the field $\psi(x,t)$ into spatial modes $g_n(x)$ and complex time dependent amplitudes $\psi_n(t)$ such as

$$\psi(x,t) = \sum_{n=-\infty}^{\infty} g_n(x)\psi_n(t). \tag{2·2}$$

The choice of the spatial basis functions will depend on the surface A and its boundary conditions, but also on practical considerations about the type of connectivity $f(x,X)$ and inputs I to the system. An adjoint basis is given by

$$\int_A dx\ \bar{g}_m(x) g_n(x) = \delta_{mn}, \tag{2·3}$$

where δ_{mn} is the Kronecker symbol. We choose a polynomial representation of the nonlinear function S in (2·1) such as

$$S(X,T) = a_0 + a_1\psi(X,T) + a_2\psi^2(X,T) + \cdots = \sum_{m=0}^{\infty} a_m \psi^m(X,T), \tag{2·4}$$

where $a_m \in \mathcal{R}$ and $I(X,T)$ is not considered (no restriction of generality). By projection of (2·1) on a spatial basis function $\bar{g}_q(x)$ and restricting its dimension N to be finite, we obtain a set of N coupled integral equations

$$\psi_q(t) = \int_A dx\ \bar{g}_q(x) \int_A dX\ f(x,X) \sum_{m=0}^{\infty} a_m \left(\sum_{n=-N}^{N} g_n(X)\psi_n(T) \right)^m . \tag{2·5}$$

Note that T still depends on the distance $|x-X|$. We perform the following trick: exchange space and time integration by introducing a time integral and a δ-function $\delta(t-\tau-v^{-1}|x-X|)$ in (2·5); then perform the integration over dX preserving $t-\tau \geq 0$ for causality. The resulting equations are

$$\begin{aligned} \Psi(t) &= v\int_{-\infty}^{t} d\tau\ \left(\Gamma_0(t-\tau) + \Gamma_1(t-\tau)\Psi(\tau) + \Gamma_2(t-\tau)\Psi(\tau)\Psi(\tau) + \cdots\right) \\ &= v\int_{-\infty}^{t} d\tau\ \Gamma_0(t-\tau) + L^t\Psi(t) + N^t(\Psi(t)), \end{aligned} \tag{2·6}$$

where vector notation has been used:

$$\Psi(t) = (\cdots \psi_q(t) \cdots)^T \tag{2·7}$$

and

$$\Gamma_0(t-\tau) = (\cdots \Gamma_q(t-\tau)\cdots)^T\ ,\ \Gamma_1(t-\tau) = (\cdots \Gamma_{qn}(t-\tau)\cdots)\ ,\cdots. \tag{2·8}$$

Formally L^t and N^t represent the linear and nonlinear temporal evolution operators. The tensor matrix elements are

$$\begin{aligned} \Gamma_q(t-\tau) &= a_0(\gamma_q^-(t-\tau) + \gamma_q^+(t-\tau)) \\ \Gamma_{qn}(t-\tau) &= a_1(\gamma_{qn}^-(t-\tau) + \gamma_{qn}^+(t-\tau)) \\ &\vdots\ , \end{aligned} \tag{2·9}$$

where

$$\begin{aligned} \gamma_q^{\pm}(t-\tau) &= \textstyle\int_A dx\ \bar{g}_q(x) f(x, x \pm v(t-\tau)) \\ \gamma_{qn}^{\pm}(t-\tau) &= \textstyle\int_A dx\ \bar{g}_q(x) f(x, x \pm v(t-\tau)) g_n(x \pm v(t-\tau)) \\ &\vdots\ . \end{aligned} \tag{2·10}$$

Our particular interest is in macroscopic phase transitions from one mode to another, i.e. the destabilization of a stationary spatiotemporal state. We consider a stationary solution Ψ_0 of (2·6) and its small deviations $\epsilon(t)$ resulting in $\Psi(t) = \Psi_0 + \epsilon(t)$. Then (2·6) may be written as

$$\begin{aligned} \epsilon(t) &= L^t\Psi(t) + N^t(\Psi(t)) - L^t\Psi_0 + N^t(\Psi_0) \\ &= \tilde{L}^t\epsilon(t) + \tilde{N}^t(\epsilon(t)), \end{aligned} \tag{2·11}$$

where $\tilde{N}^t(\epsilon(t))$ is of the order $|\epsilon|^2$. The general solution of the linear parts of (2·11) is

$$\epsilon(t) = \sum_{n=1}^{N}\left(\sum_{m=0}^{M-1} c_{mn}t^m\right) e^{\lambda_n t} O_n, \tag{2·12}$$

where c_{mn} is a constant, λ_n the eigenvalue, M its multiplicity and O_n the right-hand eigenvector. The eigenvalue problem of (2·11) is defined as

$$\det(e^{-\lambda t}L^t(e^{-\lambda\tau}) - I) = 0 \tag{2·13}$$

and provides λ_n. The identity matrix is I. Decomposing $\epsilon(t) = \sum_{i=1}^N \xi_i(t) O_i$ and defining the left-hand eigenvectors $\bar{O}_k$ of the linear problem in (2·11) we obtain by projecting (2·11) on $\bar{O}_k$

$$\xi_k(t) = \int_{-\infty}^t \lambda_k \xi_k(\tau) d\tau + \bar{O}_k \tilde{N}^t \left(\sum_{i=1}^N \xi_i(\tau) O_i \right). \tag{2·14}$$

The nonlinear contributions can be rewritten such that

$$\xi_k(t) = \int_{-\infty}^t d\tau \left(\lambda_k \xi_k(\tau) + \sum_{rs=1}^N \bar{\Gamma}_{2krs}(t-\tau) \xi_r(\tau) \xi_s(\tau) + \text{higher orders} \right) \tag{2·15}$$

with

$$\bar{\Gamma}_{2krs}(t-\tau) = \sum_{jmn=1}^N \bar{O}_k^j \Gamma_{2jmn}(t-\tau) O_r^m O_s^n, \tag{2·16}$$

where the superscript of the eigenvectors denotes their elements. Here the entire complexity of the connection topology is contained in the tensor matrices $\bar{\Gamma}$ which can be explicitly expressed as integrals of the connectivity $f(x, X)$ and the spatial basis functions $\bar{g}_n(x), g_m(x)$. The linear stability of an eigenmode $\xi_k(t)$ is determined by its eigenvalue λ_k. Thus we are able to express the entire dynamics of (2·1) in terms of its eigenmodes under appropriate choice of $\bar{g}_n(x), g_m(x)$ in the vicinity of a phase transition.

§3. Example of a two-point connection

3.1. *Analytical treatment*

Let us now consider the example of a one-dimensional homogeneous medium with a heterogeneous two-point connection between locations x_1 and x_2. The connectivity function $f(x, X)$ shall be given by

$$f(x, X) = f(|x - X|) + f_{12}(x, X) + f_{21}(x, X), \tag{3·1}$$

where f_{12} is the link from x_2 to x_1 and f_{21} the link in the opposite direction as illustrated in Fig. 1. The distance between the inhomogeneous contributions of connectivity is $d = |x - X|$ which serves as our control parameter.

The dynamics of our example is given by

$$\psi(x, t) = a \int_A dX f(x, X) S(\psi(X, T) - \bar{\psi}(X, T)) \tag{3·2}$$

with $T = t - |x - X|/v$ and $x, X \in \mathcal{R}$. $\bar{\psi}(x, t) = \int_A dX\ \psi(X, t)$ is subtracted to reduce spatially uniform saturation effects.[9),12)] Periodic boundaries are imposed. The connectivities are specified as

$$f(|x - X|) = \frac{1}{2\sigma} e^{-|x-X|/\sigma}, \qquad f_{ij}(x, X) = \frac{1}{2 f_{ij}} \delta(x - x_i) \delta(X - x_j), \qquad i \neq j, \tag{3·3}$$

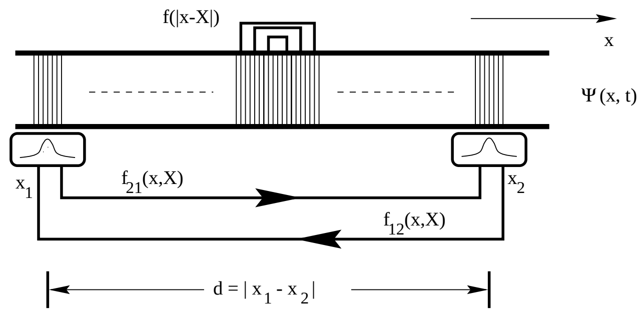

Fig. 1. Two-point connection. The homogeneous connection topology is illustrated within a one-dimensional continuous medium whose activity is described by $\psi(x,t)$. A projection from x_1 to x_2 introduces a heterogeneity into the connectivity.

where $a, \sigma, f_{12}, f_{21}$ are constant parameters. We choose the spatial basis system to be spanned by the trigonometric functions $\sin nkx, \cos mkx$ with $n, m \in \mathcal{Z}$ and $k = 2\pi/L$ where L is the length of the one-dimensional closed loop. $x_1 = 0$ is not varied thereby resulting in pinning of the spatial modes around $x = 0$. The nonlinear function S in (3·2) is assumed to be sigmoidal. [9] We study the stability of the origin $\Psi_0 = 0$ and expand S around its deflection point, $S[n] \approx \alpha n - 4/3\alpha^3 n^3 \pm \cdots$. We consider spatial basis function $g_m(x) = \cos mkx$ to 2nd order in m and truncate the expansion of the sigmoid after the 3rd order studying small amplitude dynamics. Application of (2·6)-(2·16) provides the following eigenvalue problem

$$v \int_{-\infty}^{t} d\tau \; e^{-im\omega(t-\tau)} \Gamma_{mm}(t-\tau) e^{-\lambda_m(t-\tau)} = 1, \qquad (3\cdot4)$$

where ω is a constant, m refers to the spatial mode number and

$$\Gamma_{mm}(t-\tau) = \frac{a\alpha}{\sigma} e^{-\omega_0(t-\tau)} \cos mkv(t-\tau) + d_1 \delta(|x_1 - x_2| - v(t-\tau)), \qquad (3\cdot5)$$

where

$$d_1 = 2a\alpha/L(f_{12} + f_{21}) \cos mkx_1 \cos mkx_2. \qquad (3\cdot6)$$

Inserting (3·5) in (3·4) provides us with a transcendental equation for $z = \lambda_m + im\omega$

$$\left(z^2 + 2\omega_0 z + \omega_0^2 + m^2k^2v^2\right)\left(1 - d_1 e^{zd/v}\right) - (z + \omega_0)\omega_0 a\alpha = 0. \qquad (3\cdot7)$$

The real part λ_m of the eigenvalue z of the m-th mode and its frequency ω can be determined graphically from (3·7) as a function of the control parameter d. The destabilization of a particular state m depends on d_1 and d. For $d_1, d = 0$ the purely homogeneous system is obtained in which the origin is the only stable state for sufficiently small α. The introduction of a heterogeneous projection $f_{ij}(x, X)$ may cause a desynchronization of the connected areas and thus a destabilization of the respective spatial mode resulting in a phase transition. The desynchronization properties are determined by the tensor matrices in (2·10) which describe the interplay of the connectivity and distribution of areas represented as spatial modes. This interplay prescribes the timing relationship of activity between areas via the time delay and thus determines its desynchronizing properties.

3.2. *Numerical treatment*

In Fig. 2 we investigate (3·2) numerically, we prepare the system in a well-defined state and change the connection topology by decreasing the control parameter $d = |x_1 - x_2|$. Initially the system is prepared in a coherent oscillatory stationary state. Then the connectivity is changed by moving the terminal of the inhomogeneity at $x_2 = B$ to a new location $x_2 = C$, whereas the other terminal stays constant at $x_1 = A$. The change in the connection topology destabilizes the initial stationary dynamics and the system undergoes a transition to a new stationary state via a Hopf bifurcation. Without the inhomogeneous connections the zero-activity state is stationary and stable. The parameters used for the integration of (2·1) are $v = 3, L = \pi, a = 2.5, \sigma = 0.7, \sigma_1 = \sigma_2 = 0.1, f_{12} = f_{21} = 1$. The time step is $dt = 0.02$, the space is divided into 100 units.

In Fig. 3 we investigate the dynamics in more detail by varying the control parameter d systematically from 0 to its maximal value $d = L$. Due to the periodic boundary conditions, a value $d > L/2$ reduces the relative distance between the inhomogeneities. The inhomogeneity at x_1 is kept constant; $x_2 = x_1 + d$ is varied. For each distance d the system dynamics becomes stationary and then the spatial pattern at maximum amplitude is extracted and plotted over d in a bifurcation plot. These patterns are normalized with respect to the largest amplitude. Under variation of d the system undergoes a series of spatiotemporal bifurcations. Note that these patterns are not harmonic due to the inhomogeneous connection topology. Shifts in the frequency spectra (plotted on the right for all distances d) are observed, even though the spatial pattern remains qualitatively the same. Hysteresis effects are

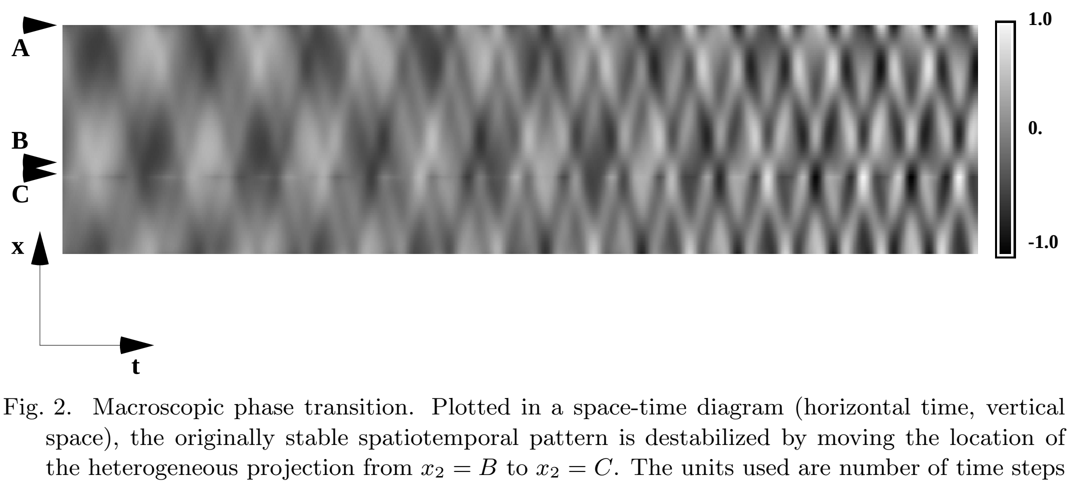

Fig. 2. Macroscopic phase transition. Plotted in a space-time diagram (horizontal time, vertical space), the originally stable spatiotemporal pattern is destabilized by moving the location of the heterogeneous projection from $x_2 = B$ to $x_2 = C$. The units used are number of time steps and arbitrary amplitude, respectively.

found resulting in an asymmetry of the bifurcation path below and above $d = L/2$. Above the bifurcation plot the corresponding amplitude (full circles) of the location x_1 and its temporal frequency are plotted (donuts) over d.

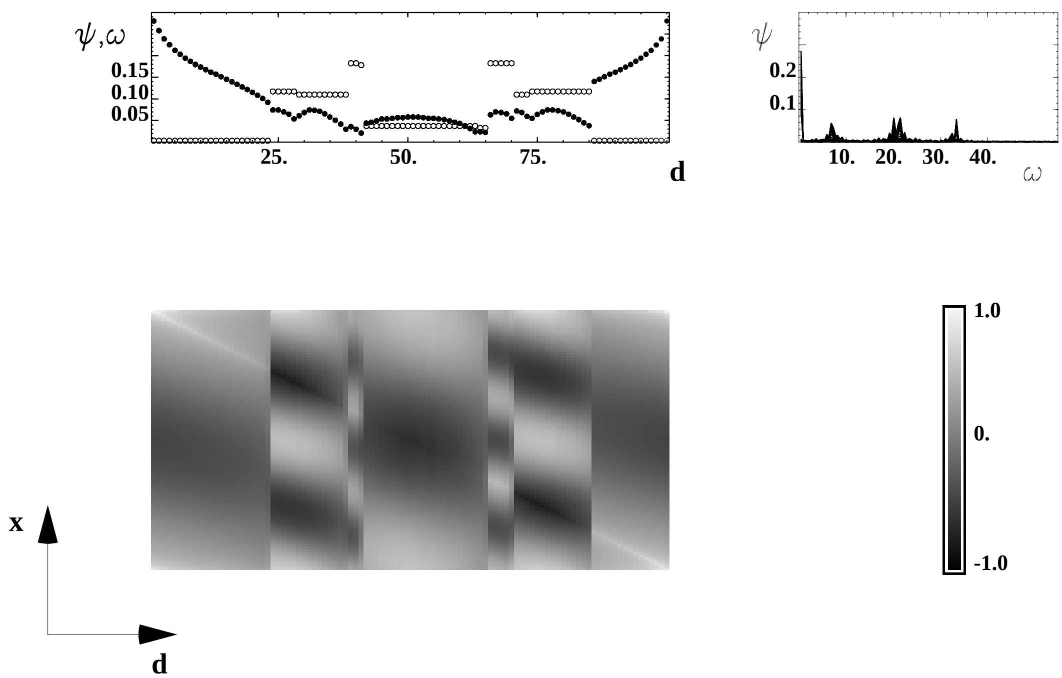

Fig. 3. Spatiotemporal bifurcation plot. The dominant spatial patterns for varying d are displayed in a spatiotemporal bifurcation diagram. Directly above, the amplitude (full circles) and temporal frequency (donuts) of the dominating pattern are plotted over the distance d. In the top right corner the power spectra of the dominating patterns are plotted for all values of d.

§4. Dimension reduction of mode equations

In §2 we reduced the spatiotemporal dynamics of a retarded nonlinear integral equation to a set of mode equations (2·15) which are linearly decoupled. The heterogeneous connection topology is completely captured by the translationally invariant integral kernels $\Gamma(t-\tau)$. Note that $\Gamma(t-\tau)$ shall represent here a tensor matrix of any order. By changing the connection topology phase transitions can be induced as shown in §3 for the variation of a two-point connection. Such a phase transition is caused by a destabilization of the initial state which is described by typically one eigenvalue λ_k crossing the imaginary axis. For ordinary differential equations dynamic systems' theory [1), 13) - 15)] says that the local center manifold theorem becomes applicable and a hierarchy of time scales emerges which leads to a dimension reduction of the pattern forming system. The dimension reduction via the center manifold theorem is one realization of Haken's slaving principle for ordinary differential equations. In the following we will show how similar principles apply to integral systems with heterogeneous connection topologies.

The variables ξ_k in (2·15) shall be grouped together in a set of slow variables $\{u_i\}$ with $\mathrm{Re}\lambda_i \approx 0$ and a set of fast variables $\{s_j\}$ with $\mathrm{Re}\lambda_j < 0$ where $|\lambda_j| \gg |\lambda_i|$. For reasons of simplicity we consider a representative of each group, i.e. $u = u_i$ and $s = s_j$, and focus on the following particular nonlinearities

$$u(t) = \int_{t_0}^{t} d\tau \ \left(\lambda_u u(\tau) + \bar{\Gamma}_{22u}(t-\tau) u(\tau) s(\tau) + \cdots\right), \tag{4·1}$$

$$s(t) = \int_{t_0}^{t} d\tau \ \left(\lambda_s s(\tau) + \bar{\Gamma}_{21s}(t-\tau) u(\tau) u(\tau) + \cdots\right) \tag{4·2}$$

neglecting higher orders of polynomials. The initial time point is t_0. For $\bar{\Gamma}_{22u}(t-\tau), \bar{\Gamma}_{21s}(t-\tau) = const$ the system represents the well-known Haken-Zwanzig model. [1] From the previous sections in the present manuscript we know that heterogeneous connection topologies manipulate the Γ tensor matrices under preservation of its translational time invariance. By solving explicitly for its linear contribution we can rewrite (4·2) as

$$s(t) = s_0 e^{\lambda_s(t-t_0)} + \int_{t_0}^{t} dT \ \left(e^{\lambda_s(t-T)} \frac{d}{dT} \int_{t_0}^{T} d\tau \ \left(\bar{\Gamma}_{21s}(T-\tau) u(T) u(T)\right)\right), \tag{4·3}$$

where s_0 specifies the initial condition at time $t = t_0$. For the long time behavior, $t_0 \longrightarrow -\infty$, the first term vanishes and we obtain an explicit (though still containing operators) representation of the dynamics of $s(t)$ in terms $u(t)$. Integrating (4·3) in parts a simpler formulation is obtained by

$$s(t) = \int_{t_0}^{t} d\tau \ u(\tau)^2 \left(\bar{\Gamma}_{21s}(t-\tau) + \lambda_s \int_{\tau}^{t} dT \ e^{\lambda_s(t-T)} \bar{\Gamma}_{21s}(T-\tau)\right). \tag{4·4}$$

Successive integration in parts of (4·4) yields

$$s(t) = \int_{t_0}^{t} d\tau \ u(\tau)^2 \left(\bar{\Gamma}_{21s}(t-\tau) + \sum_{k=0}^{n} \frac{1}{\lambda_s^k} \left(\bar{\Gamma}_{21s}^{(k)}(0) e^{\lambda_s(t-\tau)} - \bar{\Gamma}_{21s}^{(k)}(t-\tau)\right) + E(t-\tau)\right), \tag{4·5}$$

where E is the error term given by

$$E(t-\tau) = \frac{1}{\lambda_s^n} \int_{\tau}^{t} dT \ e^{\lambda_s(t-T)} \bar{\Gamma}_{21s}^{(n+1)}(T-\tau), \qquad |\lambda_s| \gg |\lambda_u|. \tag{4·6}$$

The term $\bar{\Gamma}_{21s}^{(k)}(t-\tau)$ denotes the k-th derivative with respect to t.

4.1. *Approximation via time scale hierarchy*

Besides the weak condition of long term behavior, Eqs. (4·4) and (4·5) are exact. We want to perform an approximation utilizing the different time scales of u and s. The dynamics of s is represented by a convolution of the form

$$s(t) = \int_{t_0}^{t} d\tau \ u(\tau)^2 g(t-\tau), \tag{4·7}$$

where $g(t-\tau)$ represents the convolution kernel given in (4·4), (4·5) and can be explicitly determined. We define the function $G(t)$ by

$$\frac{d}{dt}G(t) = \dot{G}(t) = g(t) \tag{4·8}$$

and rewrite (4·7) by integration of parts

$$s(t) = u(t)^2 \int_{t_0}^{t} d\tau\; g(t-\tau) + G(t-t_0)\left(u(t)^2 - u(t_0)^2\right) - \int_{t_0}^{t} d\tau\; g(t-\tau) 2u(\tau)\dot{u}(\tau). \tag{4·9}$$

As long as the state vector (u, s) remains sufficiently close to the origin $(0, 0)$ and the dynamics of $u(t)$ is sufficiently slow, i.e. $|\lambda_s| \gg |\lambda_u|$, then (4·9) will be approximated by

$$s(t) \approx u(t)^2 \int_{t_0}^{t} d\tau\; g(t-\tau) \quad = \quad s(u(t), t). \tag{4·10}$$

Equation (4·10) is the main result of this section. Note that it is given without proof of existence of $s(u(t), t)$, but it is strongly supported by numerical tests (see the following section 4.2). If $s(u(t), t)$ is not explicitly time dependent, i.e. $s = s(u(t))$, then (4·10) becomes equivalent to the local center manifold theorem (see e.g. Ref. 14)). As long as (4·10) is valid, the dynamics of the entire system (4·1), (4·2) is given by

$$u(t) = \int_{t_0}^{t} d\tau\; \left(\lambda_u u(\tau) + \bar{\varGamma}^{*}_{22u}(t-\tau) u(\tau)^3\right) \tag{4·11}$$

and

$$\bar{\varGamma}^{*}_{22u}(t-\tau) = \bar{\varGamma}_{22u}(t-\tau) \int_{t_0}^{t} d\tau\; g(t-\tau). \tag{4·12}$$

The dynamics of the variable s is enslaved by the dynamics of u which serves as an order parameter. Equation (4·10) is a realization of Haken's enslaving principle.

4.2. *Examples*

From the discussion in §3 we see that typical dependencies of the tensor matrices $\bar{\varGamma}$ may be exponential decay or periodicities. In the following we wish to discuss three examples to test the results from the previous section 4.1.

4.2.1. Haken-Zwanzig model

This model is obtained for the choice of

$$\varGamma_{22u}(t-\tau) = -1, \qquad\qquad \varGamma_{21s}(t-\tau) = 1 \tag{4·13}$$

in the system (4·1), (4·2). According to (4·4) the dynamics of s is expressed by

$$s(t) = \int_{t_0}^{t} d\tau\; e^{\lambda_s (t-\tau)} u(\tau)^2 \tag{4·14}$$

which can be approximated via (4·10) by

$$s(t) = -\frac{1}{\lambda_s} u(t)^2 \tag{4·15}$$

for long term behavior. In the present case (4·10) is identical to the local center manifold theorem [15] and (4·15) is identical to the result obtained from the method of adiabatic elimination. [1] The order parameter dynamics is given by

$$u(t) = \int_{t_0}^{t} d\tau \, \left(\lambda_u u(\tau) + \frac{1}{\lambda_s} u(\tau)^3 \right). \tag{4·16}$$

4.2.2. Exponential behavior of tensor matrices

The tensor matrices are given by

$$\Gamma_{22u}(t-\tau) = \frac{1}{2\tau_1} e^{-(t-\tau)/\tau_1}, \qquad \Gamma_{21s}(t-\tau) = \frac{1}{2\tau_2} e^{-(t-\tau)/\tau_2}. \tag{4·17}$$

Then the dynamics of s is given by

$$s(t) = \int_{t_0}^{t} d\tau \, \frac{1}{2\tau_2} u(\tau)^2 \left(e^{-(t-\tau)/\tau_2} - \frac{\lambda_s}{\lambda_s + 1/\tau_2} \left(e^{-(t-\tau)/\tau_2} - e^{-\lambda_s (t-\tau)} \right) \right). \tag{4·18}$$

After (4·10) the dynamics of s is given by

$$s(t) = \left(\tau_2 - \frac{1}{2} \right) u(t)^2 \tag{4·19}$$

and thus the order parameter dynamics of u by

$$u(t) = \int_{t_0}^{t} d\tau \, \left(\lambda_u u(\tau) + \frac{2\tau_2 - 1}{4\tau_1} e^{-(t-\tau)/\tau_1} u(\tau)^3 \right). \tag{4·20}$$

4.2.3. Periodic behavior of tensor matrices

Here the tensor matrices are given by

$$\Gamma_{22u}(t-\tau) = \frac{1}{2\tau_1} e^{-(t-\tau)/\tau_1}, \qquad \Gamma_{21s}(t-\tau) = \sin(t-\tau). \tag{4·21}$$

The dynamics of s is given by

$$s(t) = \int_{t_0}^{t} d\tau \, \frac{1}{\lambda_s^2 + 1} u(\tau)^2 \left(\sin(t-\tau) - \lambda_s \cos(t-\tau) + \lambda_s e^{-\lambda_s (t-\tau)} \right). \tag{4·22}$$

For long time behavior the approximated dynamics of s is

$$s(t) = -\frac{u(t)^2}{\lambda_s^2 + 1} \left(\cos(t-t_0) + \lambda_s \sin(t-t_0) \right) \tag{4·23}$$

and thus the order parameter dynamics of u by

$$u(t) = \int_{t_0}^{t} d\tau \, \left(\lambda_u u(\tau) - \frac{u(\tau)^3}{2\tau_1(\lambda_s^2+1)} \left(\cos(t-t_0) + \lambda_s \sin(t-t_0) \right) \right). \tag{4·24}$$

In all three examples 4.2.1-4.2.3 the numerical tests show the validity of the approximation (4·10) under the required conditions.

§5. Summary

We described macroscopic coherent pattern formation in a spatially continuous system by means of an integral equation to capture effects caused by a heterogeneous connection topology. The connectivity serves as an intrinsic topological control parameter which systematically controls spatiotemporal bifurcations. In biological systems changes in the connectivity correspond to changes in the timing behavior of cell ensembles. Particularly in the brain, these mechanisms occur when learning alters the weight of connections, or myelination along nerve axons increases the propagation velocity of action potentials and thus alters the timing between cells. The heterogenous connection topology of such systems requires a description by means of nonlinear integral equations. Utilizing a spatial mode decomposition we reduced this system to nonlinearly coupled convolution equations. In the neighborhood of a phase transition we showed how a dimension reduction of the entire system can be achieved in terms of the hypothesis given by (4·10). For the case of constant convolution kernels, our hypothesis reduces to the local center manifold theorem.

Acknowledgements

This research has been supported by NIMH and The Human Frontiers Science Project. VKJ wishes to thank Hermann Haken for interesting and helpful discussions during the 4th International Summer School in Maribor, Slovenia in 1999.

References

1) H. Haken, *Synergetics. An Introduction* (3rd ed., Springer, Berlin, 1983).
2) M. C. Cross and P. C. Hohenberg, Rev. Mod. Phys. **65** (1993), 851.
3) M. Hendrey, E. Ott and T. M. Antonsen Jr., Phys. Rev. Lett. **82** (1999), 859.
4) G. B. Ermentrout and N. Kopell, SIAM J. Appl. Math. **54** (1994), 478.
5) V. K. Jirsa, J. A. S. Kelso and A. Fuchs, Soc. f. Neurosc. **25** (1999), 898.4.
6) V. K. Jirsa and J. A. S. Kelso, submitted to Phys. Rev. Lett. (1999).
7) S. Amari, Biol. Cybern. **27** (1977), 77.
8) P. L. Nunez, *Neocortical Dynamics and Human EEG Rhythms* (Oxford University Press, 1995).
9) V. K. Jirsa and H. Haken, Phys. Rev. Lett. **77** (1996), 960.
10) J. J. Wright and D. T. J. Liley, Behav. Brain. Sci. **19** (1996), 285.
11) P. A. Robinson, C. J. Rennie and J. J. Wright, Phys. Rev. **E56** (1997), 826.
12) V. K. Jirsa, A. Fuchs and J. A. S. Kelso, Neural Comp. **10** (1998), 2019.
13) J. Guckenheimer and P. Holmes, *Nonlinear Oscillations, Dynamical Systems and Bifurcations of Vector Fields* (3rd ed., Springer, New York, 1983).
14) J. Hale and H. Kocak, *Dynamics and Bifurcations* (Springer, New York, 1991).
15) L. Perko, *Differential Equations and Dynamical Systems* (Springer, New York, 1991).